ELSEVIER

Polymer 44 (2003) 3009–3019

polymer

www.elsevier.com/locate/polymer

Re-examination of the miscibility behavior of SMMA copolymers using various techniques

S. Zhu, D.R. Paul*

Center for Polymer Research, Department of Chemical Engineering and Texas Materials Institute, The University of Texas at Austin, Austin, TX 78712-1065, USA

Received 1 November 2002; received in revised form 20 February 2003; accepted 21 February 2003

Abstract

The phase behavior of blends of SMMA copolymers with other SMMA copolymers of different compositions, with monodisperse PS homopolymers, and with monodisperse PMMA homopolymers was studied using static light scattering to assess the state of miscibility at three different temperatures: 120, 150, and 180 °C. Contrary to prior reports, the phase diagrams were found to be consistent with the binary interaction model. Quantitative evaluation of the binary interaction energy density between S and MMA, $B_{S/MMA}$, was made at each temperature by analyzing the miscibility data using the copolymer/critical molecular weight and copolymer composition mapping methods. Values of $B_{S/MMA}$ determined by two different approaches agree well. The slight temperature dependence of $B_{S/MMA}$ is well described by the Sanchez–Lacombe lattice fluid theory using a constant bare interaction energy $\Delta P^*_{S/MMA}$ by considering the temperature dependence of the characteristic parameters for PS and PMMA. Quantum mechanical calculations of the total partial charges for different triads clearly show that the electrostatic charge distribution within S and MMA repeat units remains almost unchanged as their neighboring segments change chemical identity. The experimental and theoretical results are inconsistent with the so-called 'screening', 'asymmetric miscibility' or sequence distribution effects.

Keywords: SMMA copolymer; Binary interaction model; Screening effects

1. Introduction

The binary interaction model uses a mean field approximation to describe the pair-wise interactions that occur between the repeat units in blends of different polymers or copolymers [1–3]. An essential assumption of this model is that the binary interaction energy density between repeat units i and j, B_{ij}. is not a function of copolymer sequence distribution or composition. The binary interaction model has proved quite successful for describing the phase behavior of blends based on copolymers, at least when strong specific interactions are absent [4]. Nevertheless, there are some reported exceptions to the behavior expected from this model. For example, some limited experimental work suggests that styrene (S)/methyl methacrylate (MMA) random copolymers, or SMMA, containing roughly equal amounts of S and MMA are more miscible with PMMA than with PS, a phenomena referred to as 'asymmetric miscibility' [5–8]; this suggests there is a more favorable interaction between S and MMA in SMMA/PMMA blends than in SMMA/PS blends. From the reported observations of miscibility or immiscibility and molecular weight information in these papers, it is possible to calculate an upper limit of the interaction energy between S and MMA, $B_{S/MMA}$, if the blend is miscible or a lower limit if the blend is immiscible. Our calculations reveal some inconsistencies in the limits calculated from the reported observations that suggest re-examining this behavior in a more systematic way. Braun et al. also reported some unusual results [9,10], see Fig. 1 [11], for blends of two SMMA copolymers having different copolymer compositions. The miscibility region reported is not consistent with a single value of $B_{S/MMA}$ as expected from the binary interaction model; the expected miscibility region would be two parallel lines when the copolymers have fixed molecular weights. The observations by Braun et al. have prompted a series of alternate interpretations

* Corresponding author. Tel.: +1-512-471-5392; fax: +1-512-471-0542.
E-mail address: drp@che.utexas.edu (D.R. Paul).

0032-3861/03/$ - see front matter © 2003 Elsevier Science Ltd. All rights reserved.
doi:10.1016/S0032-3861(03)00209-X

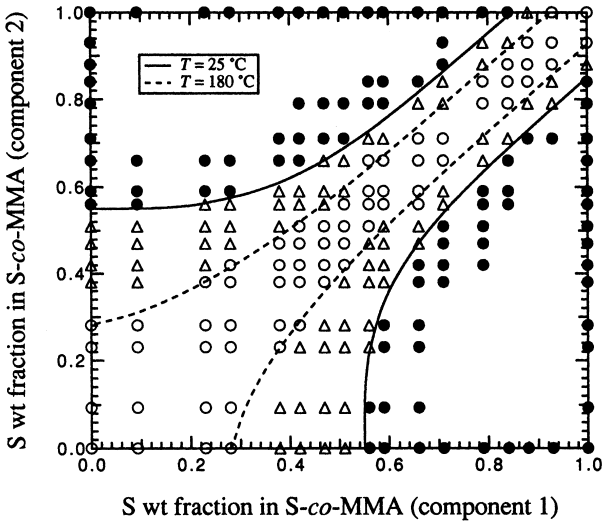

Fig. 1. Miscibility map for mixtures of two SMMA random copolymers as reported by Braun et al: (○) miscible at 25 and 180 °C; (△) miscible at 25 °C but immiscible at 180 °C; (●) immiscible at 25 and 180 °C. Lines were calculated by screening theories employing various adjustable parameters. (Reproduced from Ref. [11] with permission of the American Chemical Society).

based on sequence distribution issues and/or a so-called 'screening' effect [11–16]. It was suggested that the π electron cloud of the phenyl ring of the styrene unit might be screened by the COO group in MMA [9] such that the interaction energies are affected by the neighboring segment. This would undermine a major premise of the binary interaction model, i.e. that interactions are independent of sequencing of monomers in the chain. This is a very important issue since it implies that the binary interaction model may not apply for some copolymer systems even when strong specific interactions are not present.

One goal of this paper is to explore in depth the issue of sequence distribution/screening/asymmetric miscibility mentioned above using a combination of experimental and theoretical methods. In this study, the copolymer–copolymer phase diagram for blends of two SMMA copolymers with different compositions in Fig. 1 [11] is re-examined using more reliable techniques for assessment of blend miscibility or immiscibility. Braun and co-workers employed differential scanning calorimetry (DSC) and light microscopy to evaluate blend miscibility [9,10]; thermal analysis is compromised by the fact that the glass transition temperatures (T_g) of PS and PMMA are so close together. We then use the copolymer/critical molecular weight technique recently described [17–20] to probe the interaction energy between S and MMA. In this technique, both PMMA and PS monodisperse homopolymers of varying molecular weights are blended with SMMA copolymers of different compositions to give a more systematic assessment of the phase behavior of SMMA copolymers. In some prior reports [5–8], selected SMMA copolymers were blended with a few PS or PMMA homopolymers of different molecular weights. The copolymer/critical molecular weight technique used here should be quite informative about any anomalies or asymmetry in the S/MMA system since the plots suggested by the copolymer/critical molecular weight method will not be a straight line if such sequence distribution/screening/asymmetric miscibility effects exist. We then proceed to employ quantum mechanical calculations to determine the electrostatic total partial charge distributions within the repeat units of S and MMA for different adjacent monomer unit configurations. A basic premise of the binary interaction model for copolymer systems is that the interactions of a repeat unit with other units are independent of the chemical nature of its neighbors in the chain [4]. This will not be possible if the chemical identity of the neighbors alter the electrostatic charge distributions within this repeat unit. In other words, the charge distribution within S and MMA repeat units should be almost the same, regardless of the sequence distribution in S/MMA system, if the binary interaction model is applicable; conversely, these partial charges should be quite different if sequence distribution/screening/asymmetric miscibility effects exist.

The interaction between S and MMA units is of particular interest because of the importance of blends involving these units. The literature contains reports on the Flory–Huggins based interaction energy for the S/MMA pair, $B_{S/MMA}$, over the past half century including several in the last decade from this laboratory [4]. The reported values of $B_{S/MMA}$ vary from 0.04 to 0.34 cal/cm^3 [21,22]. Another objective of this study is to compare values of $B_{S/MMA}$ determined by copolymer composition mapping with that from the copolymer/critical molecular weight methods and to explore the temperature dependence of this interaction.

2. Background and theory

The strategies used here to determine the binary interaction energy density requires an appropriate thermodynamic theory of mixing to model the Gibbs free energy of mixing per unit volume (Δg_{mix}). The Flory–Huggins (FH) theory for a blend of monodisperse homopolymers A and B can be written as [23,24]

$$\Delta g_{mix} = B\phi_A\phi_B + RT\left[\frac{\rho_A\phi_A \ln \phi_A}{M_A} + \frac{\rho_B\phi_B \ln \phi_B}{M_B}\right] \quad (1)$$

where R is the universal gas constant, T is the absolute temperature, and ϕ_i, ρ_i and M_i are the volume fraction, density, and molecular weight of component i, respectively, and B is the desired binary interaction energy density; B is an excess free energy term that includes the contributions of the heat of mixing plus any other non-combinatorial effects. The interaction energy density B is related to the FH interaction parameter χ by $B = \chi RT/V_{ref}$, where V_{ref} is an arbitrary reference volume. Stone and Sanchez recently gave new insights about why the FH model is more useful than is generally recognized even though far more

sophisticated theories are rapidly evolving [25]. The critical interaction energy at the boundary between miscibility and immiscibility, where the energy and entropy terms in Eq. (1) are balanced, is given by the following expression

$$B_{\text{critical}} = \frac{RT}{2}\left(\sqrt{\frac{\rho_A}{(\bar{M}_W)_A}} + \sqrt{\frac{\rho_B}{(\bar{M}_W)_B}}\right)^2 \tag{2}$$

where $(\bar{M}_W)_i$ is the weight average molecular weight of polymer i. This form adequately accounts for polydispersity effects for polymers with typical molecular weight distributions [21,26–30].

For a blend of two SMMA copolymers with different compositions of interest here, the binary interaction model can be simply written as

$$B = (\phi_S' - \phi_S'')^2 B_{S/MMA} \tag{3}$$

where ϕ_S' and ϕ_S'' are the volume fractions of S in two SMMA copolymers of different compositions. The copolymer composition mapping method uses Eq. (3) combined with an appropriate, thermodynamic theory such as Eq. (1). This method is quite useful, as we have noted previously, with relatively good accuracy provided that an appropriate fitting algorithm is employed [20].

Another approach to determine the interaction energy density, called the copolymer/critical molecular weight method [17–20], combines the copolymer composition mapping method and the so-called critical molecular weight method [21,31–33]. In this paper, blends of monodisperse homopolymers of PS or PMMA with SMMA copolymers of different compositions are investigated by this approach. For these two blend systems, Eq. (3) can be simplified to

$$B = B_{S/MMA}\phi_{MMA}^2 \tag{4}$$

$$B = B_{S/MMA}\phi_S^2 \tag{5}$$

where B represents the net interaction energy density for each blend system, ϕ_{MMA} is the volume fraction of MMA in the SMMA copolymer, and ϕ_S is the volume fraction of S in the SMMA copolymer, respectively. The equations that describe the boundary between miscibility and immiscibility at a given temperature are obtained by combining either Eqs. (2) and (4) or (5), i.e.

$$\phi_{MMA} = \sqrt{\frac{B_{\text{critical}}}{B_{S/MMA}}} \tag{6}$$

$$\phi_S = \sqrt{\frac{B_{\text{critical}}}{B_{S/MMA}}} \tag{7}$$

Thus, a plot of ϕ_{MMA} (or ϕ_S) versus $\sqrt{B_{\text{critical}}}$ leads to a diagram where miscible blends are separated from the immiscible blends by a straight line passing through the origin with a slope of $1/\sqrt{B_{S/MMA}}$. Due to its advantages of simplicity and accuracy, it has been the focus of our recent interest [17–20]. However, it should be noted that only positive binary interaction energies can be determined by this method, and for very low molecular weight homopolymers end groups can become an issue [21].

Unlike the Flory–Huggins theory, equation-of-state (EOS) theories include the effects of compressibility and, thus, account for the temperature dependence of the FH based interaction energy arising from volumetric contributions; of course, other factors may contribute to the temperature dependence of the observed FH based interaction energy. In this study, the lattice fluid (LF) theory developed by Sanchez and Lacombe is used to account for the temperature dependence of the FH based interaction energy, $B_{S/MMA}$, due to its versatility and simplicity [25,34–36].

The interaction parameters, B, in the Flory–Huggins framework can be translated into the bare interaction energy, ΔP^*, of the Sanchez–Lacombe LF framework and vice versa by the following [21]

$$\begin{aligned} B_{12} = \tilde{\rho}\Delta P_{12}^* + \Bigg\{ & [P_2^* - P_1^* + (\phi_2 - \phi_1)\Delta P_{12}^*] \\ & + \frac{RT}{\tilde{\rho}}\left(\frac{1}{r_1^0 v_1^*} - \frac{1}{r_2^0 v_2^*}\right) \\ & - RT\left(\frac{\ln(1-\tilde{\rho})}{\tilde{\rho}^2} + \frac{1}{\tilde{\rho}}\right)\left(\frac{1}{v_1^*} - \frac{1}{v_2^*}\right)\Bigg\}^2 \\ & \Bigg/\left\{\frac{2RT}{v^*}\left[\frac{2\ln(1-\tilde{\rho})}{\tilde{\rho}^3} + \frac{1}{\tilde{\rho}^2(1-\tilde{\rho})} + \frac{(1-1/r)}{\tilde{\rho}^2}\right]\right\} \end{aligned} \tag{8}$$

As mentioned earlier, the mean field approximation fails if the chemical identity of the neighboring repeat units significantly alters the charge distribution within this unit. This naturally prompts us to calculate the total partial charges for each atom in the repeat unit. Sandler and Wu have demonstrated by quantum mechanical calculations that group contribution approaches to predict phase equilibria of small molecule mixtures require that the partial charge of the group be essentially independent of the nature of the rest of the molecule to which it is attached [37,38]. They used ab initio quantum mechanical calculations to determine electrostatic charges [37,38]. The less computationally intensive method of Gasteiger–Hückel (GH) was employed in this study to perform the calculation [39–43]. Partial atomic charges are calculated from orbital electronegativities by consideration of the bond structure (connectivity) of the molecule. This method assumes that the electrostatic charge of an atom is the sum of the charges due to its σ and π bonds. The method of partial equalization of orbital electronegativity (PEOE) is used to calculate the σ charge distribution. On the other hand, partial equalization of π-electronegativity (PEPE) is used to calculate partial atomic charges in π systems; the calculation is done by generating all valence bond (resonance) structures for this system and then weighting them on the basis of π-orbital electronegativities and formal considerations. The GH

method does not take the conformation of the molecule into account as noted previously [41–43]. Therefore, the atomic charges and the group charges obtained using the GH method and Sandler and Wu's approach are not quantitatively consistent. As Ziaee and Paul have demonstrated [41–43], a group (or atom) with overall charges as large as ±0.05 electron units (EU) may be considered as electroneutral in Sandler and Wu's approach, while the corresponding charges obtained using the GH method can be as large as ±0.09 EU.

3. Experimental

3.1. Materials

The monomers MMA and S were purchased from Aldrich; they were washed with an aqueous sodium hydroxide solution, rinsed with distilled water, and then dried over calcium chloride. Polymers were synthesized by addition polymerization in bulk with AIBN as the initiator at 60 °C. The reaction times were adjusted to keep the conversion less than 5% to avoid significant composition drift in the copolymer. All SMMA copolymers were recovered by addition of an excess of methanol to the reaction mixture, purified by repeated dichloromethane/methanol reprecipitation, and dried in a vacuum oven for 1 week before characterization.

The SMMA copolymers synthesized in this study are listed in Table 1. The comonomer compositions of these copolymers were determined by ^{1}H NMR and elemental analysis. The results agreed very well with each other. Fig. 2 shows the copolymerization diagram of the S/MMA comonomer pair. The solid curve was calculated from the reactivity ratios $r_S = 0.605$ and $r_{MMA} = 0.489$. These values are slightly different from those reported by Braun et al. [9]. From the values of r_1 and r_2, the sequence distribution of the monomer units in these copolymers can be calculated as shown experimentally by Bovey [44]. Weight average molecular weights and polydispersities were determined by using light scattering in dilute toluene solutions and gel permeation chromatography (GPC) calibrated with polystyrene standards, respectively. The various SMMA copolymers of different compositions were blended with each other, monodisperse PS homopolymers, and monodisperse PMMA homopolymers. The PMMA and PS homopolymer standards are described elsewhere [45,46]. The density of the polymers was determined at 30 °C by a density gradient column using calcium nitrate solutions. Glass transition temperatures (T_g) were determined to characterize the synthesized copolymers using a Perkin–Elmer DSC-7 system at a scanning rate of 20 °C/min. Two scans were performed: the first scan was run up to the corresponding annealing temperature to erase thermal history and a second run was made for thermal analysis. Fig. 3 shows the onset T_g for the synthesized SMMA copolymers with the solid lines representing the prediction of the Fox equation.

Table 1
SMMA copolymers synthesized for this study

Abbreviation	wt% S[a]	$\bar{M}_W$[b]	$\bar{M}_W/\bar{M}_n$[c]	T_g (°C)
SMMA10	10.1	255,000	2.2	118
SMMA20	20.5	250,000	2.0	116
SMMA30	30.1	315,000	2.1	114
SMMA40	39.9	267,000	2.2	112
SMMA50	51.6	232,000	2.0	109
SMMA60	61.1	217,000	1.9	108
SMMA70	71.8	220,000	2.1	105
SMMA80	82.1	219,000	2.3	103
SMMA90	91.5	220,000	2.3	102

[a] Determined by NMR and elemental analysis.
[b] Determined by light scattering.
[c] Determined by GPC.

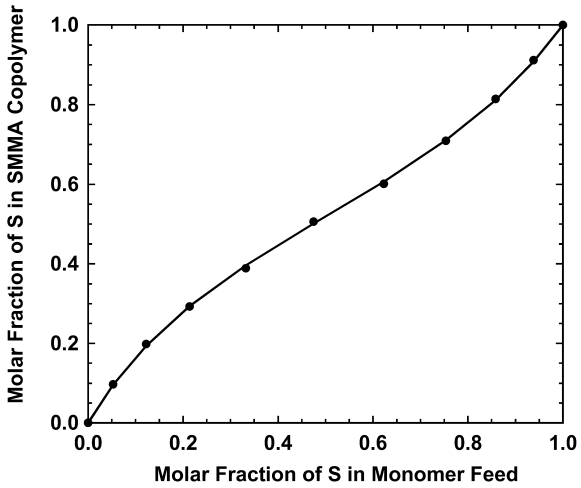

Fig. 2. Copolymerization diagram for the S/MMA system; the curve was calculated with the reactivity ratios $r_S = 0.605$ and $r_{MMA} = 0.489$.

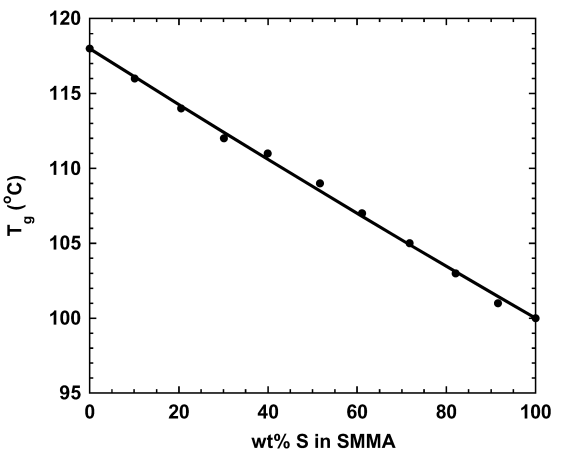

Fig. 3. Glass transition temperatures (T_g) of synthesized SMMA copolymers versus copolymer compositions. Solid lines represent the prediction of the Fox equation.

3.2. Blend preparation

Blends containing equal masses of the different copolymers (or homopolymers) were cast from 1, 2-dichloroethane solution (8 wt%) at room temperature. All blends were nearly uniform in thickness (typically 150–160 μm). These blends were then dried in a vacuum oven while increasing the temperature 20 °C every day until the designated annealing temperature was reached and thermodynamic equilibrium was further established for 1 week.

3.3. Blend assessment

Visual determination of phase behavior was made before and after the annealing treatment for each blend. Static light scattering measurements were performed for each blend. The glass transition temperatures of the blend components involved in this study were too close to each other to make a good assessment of miscibility by DSC. Nevertheless, the difference in the refractive indices between the constituent materials in this study is large enough to make a quite reliable evaluation [47]. With the aid of the combination of visual observation and light scattering measurements, the miscibility regions can be identified by optical assessment with great confidence. The light scattering apparatus used for this study is described in detail elsewhere [46]. The intensity of the static scattering from the sample using a HeNe laser light source was measured for scattering angles between 2.0° and 64.5°. A relative comparison of the maximum scattering intensity averaged at different film locations was performed to justify the optical assessment of blend miscibility.

4. Results and discussion

4.1. Re-examination of the phase diagrams for blends of SMMA copolymers of different compositions

Blends of $S_xMMA_{1-x}/S_yMMA_{1-y}(x \neq y)$ were prepared and evaluated at three different temperatures: 120, 150, and 180 °C. The isothermal miscibility phase maps obtained in this work at these temperatures for the above blends are shown in Fig. 4. In all the phase maps, the open circles represent blends found to be miscible while the filled circles represent immiscible ones. There are significant differences between the current results in Fig. 4 and those reported previously and shown in Fig. 1. These experimental differences stem from the manner in which the state of miscibility was assessed. To justify our evaluations of the phase behavior in Fig. 4, typical plots of static light scattering for two blends, SMMA10/SMMA30 and SMMA70/SMMA90, are shown in Fig. 5. The static light scattering patterns for all other blends were similar to that of either SMMA10/SMMA30 or SMMA70/SMMA90 in terms of scattering intensity.

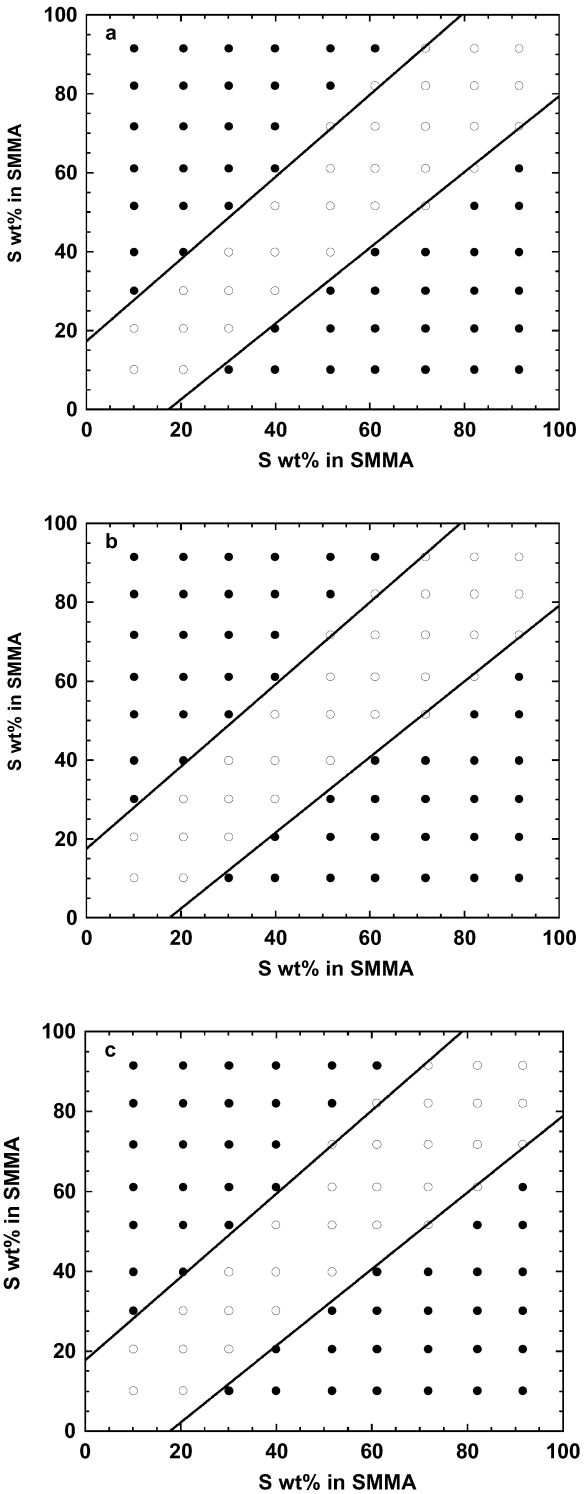

Fig. 4. Copolymer isothermal miscibility maps at (a) 120 °C; (b) 150 °C; (c) 180 °C for 50/50 blends of $S_xMMA_{1-x}/S_yMMA_{1-y}$ copolymers: (○) miscible; (●) immiscible. The $B_{S/MMA}$ values obtained from the best fit of these miscibility maps were: $B_{S/MMA} = 0.20$ cal/cm^3 at 120 °C, $B_{S/MMA} = 0.21$ cal/cm^3 at 150 °C, $B_{S/MMA} = 0.23$ cal/cm^3 at 180 °C. The solid curves were calculated from these $B_{S/MMA}$ values, respectively.

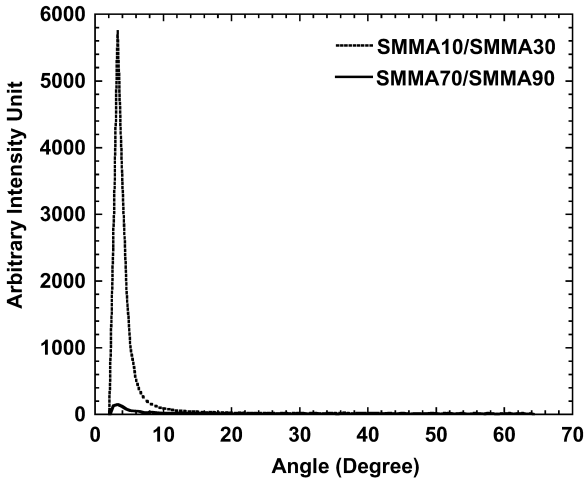

Fig. 5. Plots of the intensity of scattered light averaged at different film locations versus scattering angle in static light scattering measurements for the blends SMMA10/SMMA30 (judged immiscible) and SMMA70/SMMA90 (judged miscible).

Blends with high scattering intensity like SMMA10/SMMA30 blend were identified as immiscible while those like SMMA70/SMMA90 were judged to be miscible. The light scattering patterns of the miscible blends are essentially comparable to those of the pure component polymers; these scattered intensities for these blends and copolymers are very small on the scale shown in Fig. 5. For a number of blends, the above criteria led to a different conclusion about miscibility from that reported by Braun et al. [9,10]. For instance, blends of SMMA10/SMMA30 and SMMA70/SMMA90 were determined to be miscible and immiscible by Braun et al. [9,11], respectively. The new data in Fig. 4 suggest that the miscibility zone for blends of SMMA copolymers of different compositions, for constant temperature and fixed molecular weights of the components, is only dependent on the difference of the copolymer composition between two SMMA components in the blends, i.e. $x - y$. This is contrary to the observations in Fig. 1 where the width of the miscibility window is dependent on the copolymer compositions [9,10], i.e. x and y. Thus, the results in Fig. 4 are consistent with a constant value of the binary interaction energy between S and MMA independent of the composition of either copolymer, whereas the shape of the miscibility zone in Fig. 1 is not consistent with such a simple picture.

The data in Fig. 4 at each temperature were fitted to Eqs. (2) and (3) to obtain $B_{S/MMA}$. In the fitting process, the $B_{critical}$ value is based on the assumption of constant molecular weights of the component copolymers along the miscible boundary. The corresponding $B_{critical}$ values are 0.0072 cal/cm^3 at 120 °C, 0.0077 cal/cm^3 at 150 °C and 0.0082 cal/cm^3 at 180 °C. However, the actual $B_{critical}$ values for each copolymer–copolymer pair can be calculated from the known molecular weights and the results compared with the constant $B_{critical}$ as explained previously; a detailed analysis can be found elsewhere [48]. Deviations from the fixed $B_{critical}$ value must be considered in the fitting of interaction parameters determined in this manner as noted previously [49]. The fitting process was conducted by a computer program described elsewhere [20]. The best fit $B_{S/MMA}$ values are 0.20 cal/cm^3 at 120 °C, 0.21 cal/cm^3 at 150 °C and 0.23 cal/cm^3 at 180 °C. The solid curves in Fig. 4 were calculated using the best-fit single value of $B_{S/MMA}$. As can be seen, these curves agree well with the experimental data.

4.2. Evaluation of $B_{S/MMA}$ by the copolymer/critical molecular weight method

As demonstrated previously [19,20], the copolymer/critical molecular weight method has the advantages of potentially greater accuracy and a more direct error limit analysis compared to the copolymer composition mapping strategy. This approach provides an independent way to clarify whether so-called asymmetric miscibility or screening effects exist for the S/MMA pair or not. In the following, the value of $B_{S/MMA}$ was re-examined by this approach using data on the phase behavior of SMMA copolymers with both monodisperse PS and PMMA standards.

Miscibility data for PS/SMMA copolymer blends are plotted, in the manner suggested by Eq. (6), in Fig. 6 for 120, 150, and 180 °C where the open circles represent miscible blends and the closed circles represent immiscible blends. For the SMMA copolymers containing 17.9 wt% MMA, all blends are miscible regardless of the molecular weight of the monodiperse PS. The blends containing PS with $\bar{M}_W = 35,000$ g/mol are immiscible with SMMA copolymers containing 38.9 and more wt% MMA. The blends of the PS with $\bar{M}_W = 9000$ g/mol did not become immiscible until the MMA content was 60.1 wt%.

The same type of plot for PMMA/SMMA blends is shown in Fig. 7 for 120, 150, and 180 °C. For the SMMA copolymers containing the lowest S content (10.1 wt%), all blends are miscible regardless of the molecular weight of the monodiperse PMMA. The blends containing PMMA with $\bar{M}_W = 60,000$ g/mol were immiscible with SMMA copolymers containing 30.1 and more wt% S. The blends of the PMMA with $\bar{M}_W = 5720$ g/mol did not become immiscible until the S content was 71.8 wt%.

In these plots of ϕ_{MMA} (or ϕ_S) versus $\sqrt{B_{critical}}$, straight lines passing through the origin can be drawn that well separate the miscible from the immiscible blends, see the solid lines in Figs. 6 and 7. The error limits associated with data analysis can be estimated by constructing the dashed lines shown. Figs. 6 and 7 clearly suggest that $B_{S/MMA}$ is independent of copolymer composition since otherwise these plots would not be linear. The values of $B_{S/MMA}$ determined at a given temperature from the slopes of the lines drawn for PS/SMMA and for PMMA/SMMA blends are identical. The values are 0.21 cal/cm^3 at 120 °C,

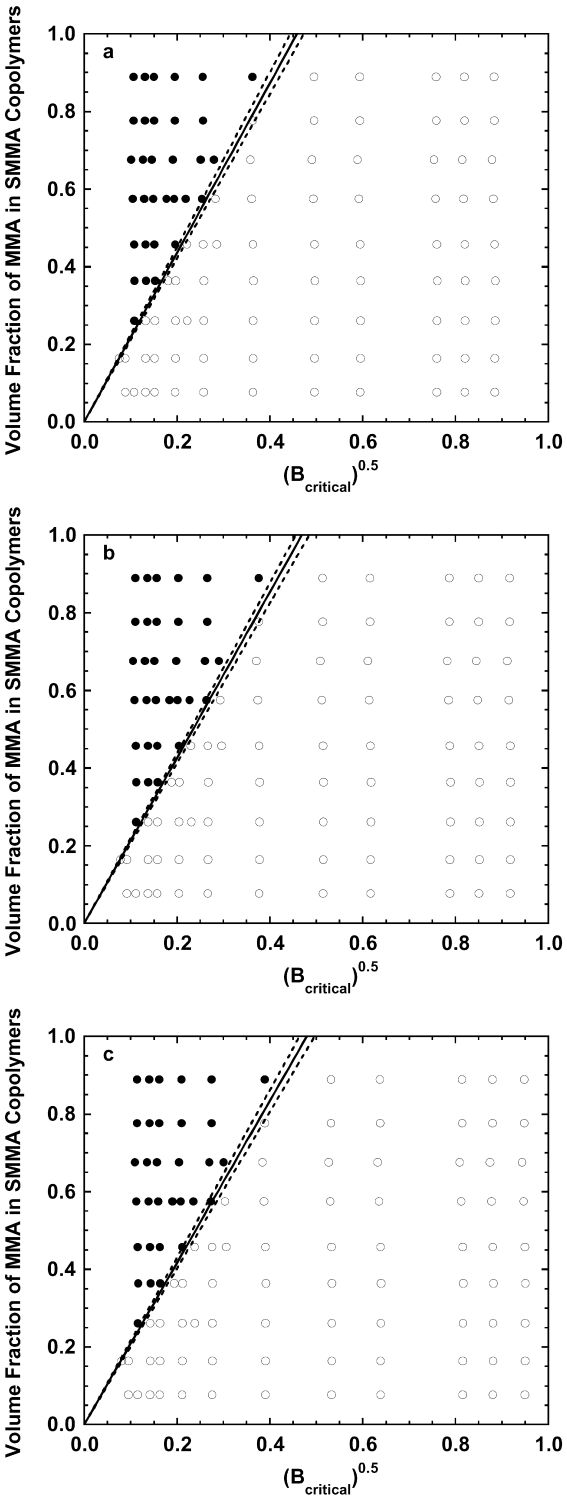

Fig. 6. Isothermal miscibility maps at (a) 120 °C; (b) 150 °C; (c) 180 °C for 50/50 blends of SMMA copolymers with PS homopolymers of varying molecular weights plotted according to Eq. (6): (○) miscible; (●) immiscible. From the slopes of the lines separating the miscible and immiscible blends, the following was calculated: $B_{S/MMA} = 0.21 \pm 0.01$ cal/cm^3 at 120 °C, $B_{S/MMA} = 0.22 \pm 0.01$ cal/cm^3 at 150 °C, $B_{S/MMA} = 0.24 \pm 0.01$ cal/cm^3 at 180 °C.

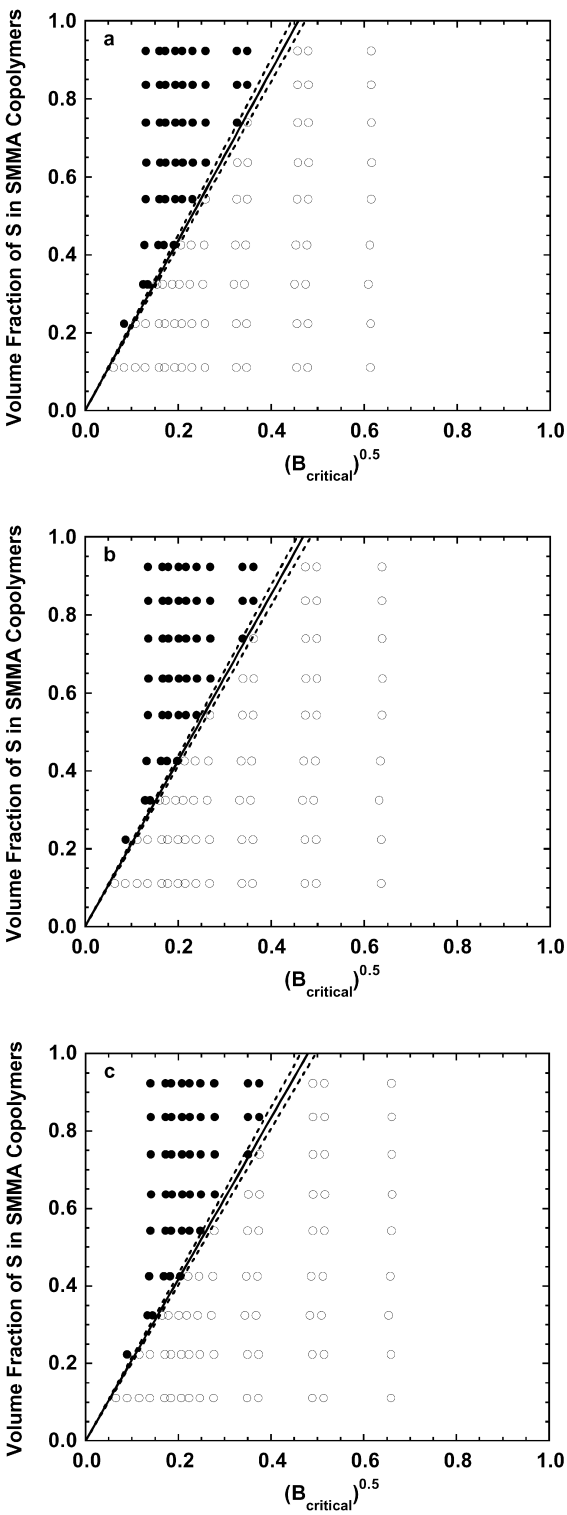

Fig. 7. Isothermal miscibility maps at (a) 120 °C; (b) 150 °C; (c) 180 °C for 50/50 blends of SMMA copolymers with PMMA homopolymers of varying molecular weights plotted according to Eq. (7): (○) miscible; (●) immiscible. From the slopes of the lines separating the miscible and immiscible blends the following was calculated: $B_{S/MMA} = 0.21 \pm 0.01$ cal/cm^3 at 120 °C, $B_{S/MMA} = 0.22 \pm 0.01$ cal/cm^3 at 150 °C, $B_{S/MMA} = 0.24 \pm 0.01$ cal/cm^3 at 180 °C.

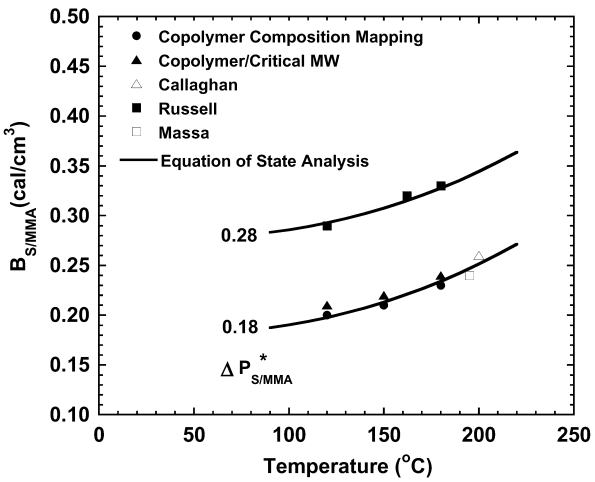

Fig. 8. Summary of $B_{S/MMA}$ values obtained from various sources (see Refs. [21,22]) including this study. The solid curves were calculated according to Eq. (8) for the values of $\Delta P^*_{S/MMA}$ shown using the temperature-dependent Sanchez–Lacombe characteristic parameters reported from Ref. [19].

0.22 cal/cm^3 at 150 °C and 0.24 cal/cm^3 at 180 °C. These values are slightly larger than those obtained earlier by the copolymer composition mapping method. Comparison with the other values reported in the literature are given in Section 4.3.

4.3. Temperature dependence of $B_{S/MMA}$

The $B_{S/MMA}$ values determined from the two approaches described above, i.e. copolymer composition mapping and copolymer/critical molecular weight methods, are plotted versus temperature in Fig. 8 along with other values from the literature [21,22,49]. The values of $B_{S/MMA}$, determined by the two current methods, agree well with each other and with the data from Massa et al. and Callaghan et al. [21,22,49]. The results from Russell, however, are substantially larger [21,22,49]; a possible explanation is offered later. All the results in Fig. 8 suggest that $B_{S/MMA}$ increases slightly with temperature. This is consistent with previous observations [21,22,49]. One explanation of the trend is that EOS effects cause this slight temperature dependence of the Flory–Huggins value of $B_{S/MMA}$. This possibility can be tested by assuming that the bare interaction energy, $\Delta P^*_{S/MMA}$, in the Sanchez–Lacombe theory is independent of temperature and then see if Eq. (8) describes how $B_{S/MMA}$ varies with temperature. The temperature-dependent Sanchez–Lacombe EOS characteristic parameters for PS and PMMA used in the calculation were taken from our prior publication [19]. As seen in Fig. 8, the temperature dependence of $B_{S/MMA}$ is well described by the Sanchez–Lacombe LF theory with a constant value of $\Delta P^*_{S/MMA}$; a value of $\Delta P^*_{S/MMA} = 0.18$ cal/cm^3 gives a curve consistent with the current data and with the data of Massa and Callaghan but a value of $\Delta P^*_{S/MMA} = 0.28$ cal/cm^3 is needed to fit the data of Russell. This plot suggests that EOS effects are primarily responsible for temperature dependence of the Flory–Huggins interaction energy as noted elsewhere [19]. Hence, to a very good approximation, the bare interaction energy between S and MMA, $\Delta P^*_{S/MMA}$, is independent of temperature. With regard to the absolute difference between the $B_{S/MMA}$ curves formed by the data from Russell and that from other sources including the current study, it is important to call attention to three points. First, the Russell data were determined by small-angle neutron scattering from block copolymers, i.e. PS-*b*-PMMA, while all of the data on the lower curves were derived from physical blends [21,22]. Second, the S blocks in the Russell study were deuterated to give contrast in neutron scattering. Deuteration is well-known to perturb the interaction energy [50–52]. This effect is likely to be much greater on a relative basis for weakly interacting systems like the S/MMA pair. Third, the interaction energies determined in this study are associated with chemical potentials while those obtained from SANS measurements are associated with the spinodal. Sanchez [53] has shown that interaction energies from these sources can be quantitatively different.

4.4. Electrostatic partial charge calculations

As mentioned earlier, the partial charge distribution could be a good indicator of whether sequence distribution/screening/asymmetric miscibility effects exist. To explore this, a quantum mechanical approach was used to calculate the electrostatic partial charge distribution within MMA and S repeat units in different MMA-centered and S-centered triad structures. The MMA-centered triads used were MMA–MMA–MMA, S–MMA–S, MMA–MMA–S and S–MMA–MMA and the results are listed in Table 2. To simplify the calculations, analogue molecules terminated with methyl groups at both ends were used to represent the corresponding triads. For example, the triad S–MMA–S was represented by the molecule shown in Fig. 9. It should be noted that we assume in our calculations that repeat units of S and MMA are connected in a head-to-tail sequence; this appears well-justified on both experimental and theoretical grounds [54]. The same kind of calculations can be

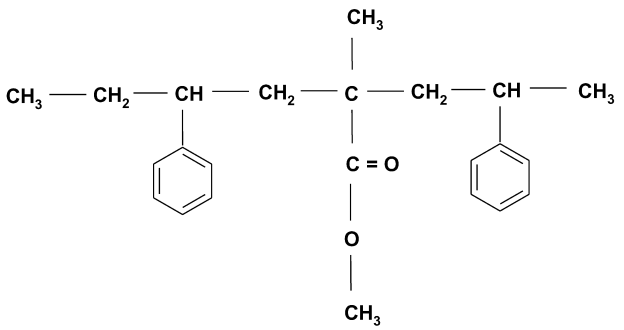

Fig. 9. Chemical structure for the analogue molecule used in the quantum mechanical calculations on the electrostatic partial charge distribution within MMA and S repeat units. This molecule, terminated with methyl groups at both ends to facilitate calculation, represents the structure for the triad S–MMA–S.

Table 2
Electrostatic charge distribution for MMA/S pair calculated by GH method

Atom or group in MMA	*Total partial electrostatic charge (EU) in different triads structure*			
	MMA–MMA–MMA	S–MMA–S	MMA–MMA–S	S–MMA–MMA
C_1	−0.02	−0.03	−0.02	−0.03
C_2	0.06	0.06	0.06	0.06
C_3	0.29	0.29	0.29	0.29
C_4	0.05	0.05	0.05	0.05
C_5	−0.05	−0.05	−0.05	−0.05
O_I	−0.38	−0.38	−0.38	−0.38
O_{II}	−0.22	−0.22	−0.22	−0.22
H_a	0.03	0.03	0.03	0.03
H_b	0.05	0.05	0.05	0.05
H_c	0.02	0.02	0.02	0.02
Ester group	−0.31	−0.31	−0.31	−0.31
MMA repeat unit	0	−0.01	0	−0.01
Atom or group in S	*Total partial electrostatic charge (EU) in different triads structure*			
	S–S–S	MMA–S–MMA	S–S–MMA	MMA–S–S
C_1	−0.04	−0.03	−0.04	−0.03
C_2	−0.01	−0.01	−0.01	−0.01
C_3	−0.04	−0.05	−0.05	−0.05
C_4	−0.06	−0.06	−0.06	−0.06
C_5	−0.06	−0.06	−0.06	−0.06
C_6	−0.06	−0.06	−0.06	−0.06
C_7	−0.06	−0.06	−0.06	−0.06
C_8	−0.06	−0.06	−0.06	−0.06
H_a	0.03	0.03	0.03	0.03
H_b	0.04	0.04	0.04	0.04
H_c	0.06	0.06	0.06	0.06
H_d	0.06	0.06	0.06	0.06
H_e	0.06	0.06	0.06	0.06
H_f	0.06	0.06	0.06	0.06
H_g	0.06	0.06	0.06	0.06
Phenyl group	−0.04	−0.05	−0.05	−0.05
S repeat unit	0	0.01	0	0.01

performed for the electrostatic charge distribution for S repeat units; the S-centered triads used were SSS, MMA–S–MMA, MMA–S–S, and S–S–MMA and the results are listed in Table 2. The atomic legends for MMA, S are shown in Fig. 10. As can be clearly seen from Table 2, for all the MMA-centered triads, the carbon atom C_1 in the MMA repeat unit experiences the most change in electrostatic charge distribution among all the atoms in MMA. For example, its total partial charge varies from −0.02 EU in triad MMA–MMA–MMA to −0.03 EU in triad S–MMA–S. However, this change is not significant since this carbon atom can still be considered as electroneutral in all triads according to the empirical criteria for electroneutrality based on the GH method [41–43]. On the other hand, the electrostatic charges for the other atoms in MMA repeat unit remain almost constant. It is especially so for the ester group in MMA. This can be understood by considering the fact that the induction effect diminishes with the number of the chemical bonds, n, and eventually is negligible when n is even greater. Similar observations can be made from Table 2 for the S repeat unit in S-centered triads. Therefore, the above quantum mechanical partial charge calculations are inconsistent with the assumption, behind the screening effects proposed by Braun et al. that the phenyl group in S is screened by the ester group in MMA. Moreover, these calculations suggest that the mean filed approximation assumption is still valid for S/MMA pair regardless of the

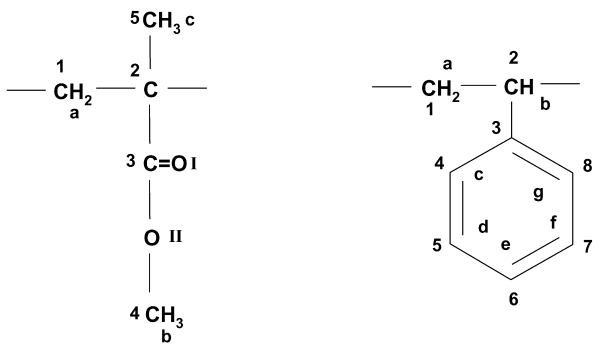

Fig. 10. Atomic legends for MMA and S repeat units used in quantum mechanical partial charge calculations by GH method. Arabic numbers (1, 2, 3, etc.), alphabetic letters (a, b, c, etc.) and Roman numerals (I, II, etc.) are assigned to represent carbon, hydrogen and oxygen, respectively.

sequence distribution since the electrostatic charge distribution within S (or MMA) repeat units is almost the same for all S-centered (or MMA-centered) triads with different adjacent chemical identities.

5. Conclusions

The equilibrium miscibility of blends of SMMA copolymers with other SMMA copolymers of different compositions, with monodisperse PS homopolymers, and with monodisperse PMMA homopolymers was determined at different temperatures using static light scattering to distinguish one phase from two phase mixtures. Contrary to prior reports, the region of miscibility for blends of S_x $MMA_{1-x}/S_yMMA_{1-y}(x \neq y)$ was found to be entirely consistent with a single interaction energy between styrene and methyl methacrylate units for all copolymer compositions and the predictions of the binary interaction model, see Fig. 4. Quantitative evaluation of the binary interaction energy density for the S and MMA repeat unit pair, $B_{S/MMA}$, was made at each temperature by analyzing the miscibility data using the copolymer/critical molecular weight and copolymer composition mapping methods. The values of $B_{S/MMA}$ determined here by the copolymer composition mapping approach are well consistent with those obtained by the copolymer/critical molecular weight strategy, see Fig. 8. This is suggested by our previous studies [20]. It again proves that the copolymer/critical molecular weight approach is a generally more accurate and convenient alternative with recognized limitations. The current values agree well with some of the results from the prior literature. There is a slight temperature dependence of $B_{S/MMA}$ which seems to be simply a result of EOS effects since this trend is well described by the Sanchez–Lacombe LF theory with a constant bare interaction energy $\Delta P^*_{S/MMA}$ but considering the temperature dependence of the characteristic parameters for PS and PMMA, see Fig. 8. Copolymer/critical molecular weight experiments for blends of SMMA with monodisperse PS and with monodisperse PMMA showed that the boundary between miscible and immiscible regions can be well separated by straight lines passing through the origin, see Figs. 6 and 7; which is strong evidence that $B_{S/MMA}$ does not depend on copolymer composition or what are the nearest neighbors of S or MMA units in the copolymer chain at a given temperature. Quantum mechanical calculations of the total partial charges for different triads clearly show that the electrostatic charge distribution of the repeat unit remains almost unchanged as the nearest neighbors change identity. These new experimental and theoretical results do not support the existence of any screening, asymmetric miscibility or sequence distribution effects for the S/MMA pair. We conclude that the binary interaction model can be used with confidence for blend systems based on these monomer units.

Acknowledgements

This research was funded by National Science Foundation grant number DMR 97-26484 administered by the Division of Materials Research-Polymers Program.

References

[1] Kambour RP, Bendler JT, Bopp RC. Macromolecules 1983;16:753.
[2] ten Brinke G, Karasz FE, MacKnight WJ. Macromolecules 1983;16:1827.
[3] Paul DR, Barlow JW. Polymer 1984;25:487.
[4] Merfeld GD, Paul DR. In: Paul DR, Bucknall CB, editors. Polymer blends: formulation and performance, vols. 1 and 2. New York: Wiley; 2000. p. 55.
[5] Kulasekere R, Kaiser H, Ankner JF, Russell TP, Brown HR, Hawker CJ, Mayes AM. Macromolecules 1996;29:5493.
[6] Galvin ME. Macromolecules 1991;24:6354.
[7] Winey KI, Berba ML, Galvin ME. Macromolecules 1996;29:2868.
[8] Pellegrini NN, Winey KI. Macromolecules 2000;33:73.
[9] Braun D, Yu D, Kohl PR, Gao X, Andradi LN, Manger E, Hellmann GP. J Polym Sci Part B: Polym Phys 1992;30:577.
[10] Kohl PR, Seifert AM, Hellmann GP. J Polym Sci Part B: Polym Phys 1990;28:1309.
[11] Hino T, Song Y, Prausnitz JM. Macromolecules 1995;28:5709.
[12] Hino T, Lambert SM, Soane DS, Prausnitz JM. Polymer 1993;34:4756.
[13] Hino T, Song Y, Prausnitz JM. Macromolecules 1994;27:5681.
[14] Hino T, Song Y, Prausnitz JM. Macromolecules 1995;28:5717.
[15] Hino T, Song Y, Prausnitz JM. Macromolecules 1995;28:5725.
[16] Song Y, Lambert SM, Prausnitz JM. Macromolecules 1994;27:441.
[17] Chu JH, Tilakaratne HK, Paul DR. Polymer 2000;41:5393.
[18] Chu JH, Paul DR. Polymer 2000;41:7193.
[19] Zhu S, Paul DR. Macromolecules 2002;35:2078.
[20] Zhu S, Paul DR. Macromolecules 2002;35:8227.
[21] Callaghan TA, Paul DR. Macromolecules 1993;26:2439.
[22] Russell TP, Hjelm Jr RP, Seeger PA. Macromolecules 1990;23:890.
[23] Flory PJ. J Chem Phys 1942;10:51.
[24] Huggins ML. J Chem Phys 1941;9:440.
[25] Stone MT, Sanchez IC. In: Paul DR, Bucknall CB, editors. Polymer blends: formulation and performance, vols. 1 and 2. New York: Wiley; 2000. p. 15.
[26] Koningsveld R, Chermin HAG, Gordon M. Proc R Soc Ser A 1970;319:331.
[27] Koningsveld R, Kleintjens LA, Schoffeleers HM. Pure Appl Chem 1974;39:1.
[28] Koningsveld R. Br Polym J 1975;7:435.
[29] Koningsveld R, Kleintjens LA. J Polym Sci, Polym Symp 1977;61:221.
[30] Salomons W, Ten Brinke G, Karasz FE. Polym Commun 1991;32:185.
[31] Kambour RP, Gundlach PE, Wang ICW, White DM, Yeager GW. Polym Commun 1988;29:170.
[32] Callaghan TA, Takakuwa K, Paul DR, Padwa AR. Polymer 1993;34:3796.
[33] Takakuwa K, Gupta S, Paul DR. J Polym Sci, Part B: Polym Phys 1994;32:1719.
[34] Sanchez IC, Lacombe RH. J Phys Chem 1976;80:2352.
[35] Sanchez IC, Lacombe RH. J Polym Sci, Polym Lett Ed 1977;15:71.
[36] Sanchez IC, Lacombe RH. Macromolecules 1978;11:1145.
[37] Wu HS, Sandler SI. Ind Engng Chem Res 1991;30:881.
[38] Wu HS, Sandler SI. Ind Engng Chem Res 1991;30:889.
[39] Gasteiger J, Marsili M. Tetrahedron 1980;36:3219.
[40] Gasteiger J, Marsili M. Org Magn Reson 1981;15:353.

[41] Ziaee S, Paul DR. J Polym Sci, Part B: Polym Phys 1996;34:2641.
[42] Ziaee S, Paul DR. J Polym Sci, Part B: Polym Phys 1997;35:489.
[43] Ziaee S, Paul DR. J Polym Sci, Part B: Polym Phys 1997;35:831.
[44] Bovey FA. J Polymer Sci 1962;62:197.
[45] Chu JH-C. PhD Dessertation. Austin: The University of Texas; 1999
[46] Merfeld GD. PhD Dessertation. Austin: The University of Texas; 1998
[47] Van Krevelen DW. Properties of polymers: their estimation and correlation with chemical structure, 2nd ed. New York: Elsevier; 1976.
[48] Zhu S. PhD Dessertation. Austin: The University of Texas; 2003
[49] Chu JH, Paul DR. Polymer 1999;40:2687.
[50] Atkin EL, Kleint'jens LA, Koningsveld R, Fetters LJ. Polym Bull (Berlin) 1982;8:347.
[51] Bates FS, Wignall GD, Koehler WC. Phys Rev Lett 1985;55:2425.
[52] Lin JL, Roe RJ. Macromolecules 1987;20:2168.
[53] Sanchez IC. Polymer 1989;30:471.
[54] Odian GG. Principles of polymerization, 2nd ed. New York: Wiley; 1981.